Genes, Brain and Behavior
Official publication of the International Behavioural and Neural Genetics Society

Genes, Brain and Behavior (2011) doi: 10.1111/j.1601-183X.2011.00719.x

rKv1.2 overexpression in the central medial thalamic area decreases caffeine-induced arousal

C. Cazzin*,†, L. Piccoli†, M. Massagrande†, N. Garbati†, F. Michielin‡, H.-G. Knaus§, C. J. A. Ring¶, A. D. Morrison¶, E. Merlo-Pich†, Z. Rovo, S. Astori**, A. Lüthi**, C. Corti† and M. Corsi†**

*† Neurosciences Centre of Excellence for Drug Discovery, ‡Clinical Pharmacology Statistics & Programming, GlaxoSmithKline, Medicines Research Centre, Verona, Italy, §Division of Molecular and Cellular Pharmacology, Department for Medical Genetics, Molecular and Clinical Pharmacology, Innsbruck Medical University, Innsbruck, Austria, ¶Molecular Discovery Research, GlaxoSmithKline, New Frontiers Science Park, Harlow, UK, and **Department of Cell Biology and Morphology, University of Lausanne, Lausanne, Switzerland*
**Corresponding author: C. Cazzin, Medicines Research Centre, Aptuit Verona S.r.l., via Fleming, 4- 37135 Verona, Italy. E-mail: cazzin-c@libero.it*

Received 7 October 2010, revised 24 June 2011, accepted for publication 11 July 2011

The voltage-gated potassium channel Kv1.2 belongs to the shaker-related family and has recently been implicated in the control of sleep profile on the basis of clinical and experimental evidence in rodents. To further investigate whether increasing Kv1.2 activity would promote sleep occurrence in rats, we developed an adeno-associated viral vector that induces overexpression of rat Kv1.2 protein. The viral vector was first evaluated *in vitro* for its ability to overexpress rat Kv1.2 protein and to produce functional currents in infected U2OS cells. Next, the adeno-associated Kv1.2 vector was injected stereotaxically into the central medial thalamic area of rats and overexpression of Kv1.2 was showed by *in situ* hybridization, *ex vivo* electrophysiology and immunohistochemistry. Finally, the functional effect of Kv1.2 overexpression on sleep facilitation was investigated using telemetry system under normal conditions and following administration of the arousing agent caffeine, during the light phase. While no differences in sleep profile were observed between the control and the treated animals under normal conditions, a decrease in the pro-arousal effect of caffeine was seen only in the animals injected with the adeno-associated virus-Kv1.2 vector. Overall, our data further support a role of the Kv1.2 channel in the control of sleep profile, particularly under conditions of sleep disturbance.

Keywords: Adeno-associated vector, Caffeine, Kv1.2, shaker channels, sleep, thalamus

The family of human Kv channels is characterized by 40 genes and is divided into 12 subfamilies (Kv1–Kv12) (Gutman *et al*. 2003). Within the family, the Kv1 subfamily presents highest homology with the *Drosophila melanogaster* voltage-gated *shaker* channel and is characterized by eight members (Kv1.1–Kv1.8). They play a central role in the physiology of excitable cells and are generally homo- or heterotetramers of α subunits associated with auxiliary β subunits (β1 and/or β2) (Trimmer & Rhodes 2004).

Among Kv1.x channels, Kv1.2 is the most highly expressed in the mammalian brain, with homogenous expression in the thalamocortical area, the reticular thalamic nuclei and the hippocampus (Trimmer & Rhodes 2004). As the rat thalamocortical system is important for the control of sleep rhythms (Steriade 2006) and Kv1.2 channel is involved in the reduction of membrane excitability, a role for Kv1.2 in regulating mammalian sleep can be hypothesized. The first experimental evidence supporting this hypothesis came from genetic studies in *Drosophila melanogaster* by Cirelli *et al*. (2005). Three different phenotypes related to the *Shaker* gene and showing strong sleep abnormalities were identified by mutagenesis screenings in *Drosophila* (Bushey *et al*. 2007; Cirelli *et al*. 2005; Koh *et al*. 2008; Wu *et al*. 2010). A functional role in sleep occurrence was further investigated through generation of Kv1.2 knock-out mice (Douglas *et al*. 2007). These animals showed an abnormal sleep pattern, with significant reduction of non-rapid eye movement (NREM) sleep duration while maintaining normal sleep homeostasis. Moreover, injection of a specific Kv1.2 antibody in adult rat cortex blocked electroencephalographic (EEG) signs of NREM sleep, and antibody microinfusion in the central medial thalamic area (CMT) temporarily restored consciousness in sevoflurane/desflurane-anesthetized rats (Alkire *et al*. 2009; Douglas *et al*. 2006). This experimental evidence suggests that the blockage of Kv1.2 currents induces a long-lasting depolarization of thalamocortical cells not allowing the occurrence of NREM sleep. On the other hand, activation of Kv1.2 in the thalamocortical area could promote occurrence of NREM sleep and therefore allowed sleep in conditions of sleep disturbance. This hypothesis suggests Kv1.2 as a potential therapeutic target for sleep disorders (Cirelli 2009; Wulff *et al*. 2009). This is also supported clinically by the central role played by the auto-antibody against Kv channels (Kv1.1, Kv1.2 and Kv1.6) in producing the severe insomnia observed in the

patients suffering from Morvan's syndrome (Kleopa *et al*. 2006; Liguori *et al*. 2001). Unfortunately, no specific positive modulators for this class of ion channels are available at present. Therefore, we developed an adeno-associated viral vector (AAV) encoding the rat Kv1.2 channel to elucidate the effect of Kv1.2 overexpression on sleep profile. The AAV2/9-Kv1.2 vector was injected into the CMT and the behavioural profile was assessed with particular focus on sleep profile in normal and disturbed conditions. Caffeine treatment was chosen to produce disturbed sleep in rats because, as reported in the literature, it produces similar symptoms of insomnia in both rats and humans (Paterson *et al*. 2009).

Materials and methods

Viral vector production and purification

An AAV vector plasmid was designed to express both enhanced green fluorescent protein (eGFP) and the rat Kv1.2 cDNA from the cytomegalovirus (CMV) immediate early (IE) promoter. The rat Kv1.2 coding sequence (NM_012970 from base 582 to 2081) was amplified from rat hippocampal cDNA and ligated into the 'Gateway'-compatible plasmid pENTR1A-eGFP-2A-*Cla*I. This placed the Kv1.2 coding sequences downstream and in-frame with plasmid sequences encoding an eGFP-2A-fusion peptide to form a single open reading frame encoding an eGFP-2A-Kv1.2 peptide. The eGFP-2A-Kv1.2 cassette was then shuttled into a modified version of the plasmid pAAVCMVpoly that acts as a Gateway destination vector, called pAAVCMVpoly_rfaGW_positive. Analysis of the resulting construct was carried out by double-stranded sequencing and by digestion with *Pvu*II and *Sma*I [to confirm integrity of the adeno-associated virus inverted terminal repeats (AAV ITRs)].

Production of AAV2/9-based vectors was performed by ReGenX (ReGenX Biosciences, Washington DC, USA) using the method described by Gao *et al*. (2002). Viral vectors were purified by cesium chloride density-gradient centrifugation and suspended in phosphate-buffered saline (PBS)/3% (w/v) sucrose, and the final viral titer was determined by TaqMan analysis.

The control virus AAV2/9-CMV-eGFP was kindly provided by the Vector Core at the University of Pennsylvania, USA.

Viral vector infections of cell culture in vitro

U2OS cells were grown in Dulbecco's modified Eagle's minimal essential medium (DMEM)/F-12 medium (Gibco, Invitrogen, Milan, Italy) with heat-inactivated 10% foetal bovine serum (Gibco) and plated at 5×10^4 cells/well in six-well plates on poly-D-lysine-treated coverslips with diameter 12 mm (BD BioCoat, Franklin Lakes, NJ USA) for immunocytochemistry and for electrophysiology study. Cells were incubated at 5% CO_2 at 37°C overnight.

The day after cell plating, U2OS cells were infected with the AAV2/9-CMV-eGFP or AAV2/9-CMV-eGFP-2A-Kv1.2 viruses at a dose of 10^4, 10^5 or 10^6 genome copies per cell (gc/cell), and Kv1.2 and GFP protein expression and Kv1.2 functional current were assessed 4 days post-inoculation by immunocytochemistry and by manual patch clamp, respectively.

Fluorescence immunocytochemistry

The coverslips were dipped in cold PBS and incubated in 100% methanol for 6 min at −20°C (Sigma-Aldrich S.r.l., Milan, Italy). After three washes in PBS, each coverslip was incubated in blocking solution [5% normal goat serum (Vector Laboratories, Burlingame, CA, USA) and 0.2% Triton-X-100 in PBS (Sigma-Aldrich S.r.l.)] for 1 h with soft agitation. Then coverslips were incubated with primary antibodies diluted in blocking solution for 2 h at room temperature in a humid atmosphere. The primary antibodies used were rabbit polyclonal Anti-Kv1.2 1:500 (Alomone Labs, Jerusalem, Israel) and mouse monoclonal anti-GFP 1:500 (Chemicon, Temecula, CA, USA).

After three washes in PBS, coverslips were incubated with the secondary antibody (anti-mouse immunoglobulin/Alexa Fluor-488 and anti-rabbit immunoglobulin/Alexa Fluor-594; Molecular Probes, Eugene, OR, USA) diluted 1:1000 in blocking solution for 1 h. Finally, each coverslip was mounted on a slide with Vectashield containing 4′,6-diamidino-2-phenylindole (DAPI) (Vector Laboratories) and the slides kept at 4°C until use.

Images were acquired with the Nikon Microphot-Fxa fluorescence microscope at the 20× magnification with the digital camera system Leica DC500 (Leica Microsystems GmbH, Mannheim, Germany) using the software Leica IM50 (Version 1.20 – release 19).

Whole-cell voltage-clamp recording from Kv1.2-expressing U2OS cells

Cells plated on the glass coverslips were positioned in a recording chamber (0.5 ml), mounted on the stage of an inverted microscope (Axiovert 135, Carl Zeiss, Milan, Italy) and superfused with an extracellular solution at a rate of 2 ml/min. The standard extracellular solution contained (in mM): 150 NaCl, 5 KCl, 1 $MgCl_2$, 2 $CaCl_2$, 5 glucose, 10 HEPES (all reagents from Sigma). The pH was adjusted to 7.4 using NaOH. Borosilicate-glass patch pipettes (WPI, Sarasota, FL, USA) were pulled using a Sutter P-97 electrode puller and filled with an internal solution consisting of (in mM): 70 KCl, 65 KF, 5 NaCl, 1 $MgCl_2$, 10 ethyleneglycoltetraacetic acid (EGTA) and 10 HEPES . The pH was adjusted to 7.3 using KOH. In the first set of experiments, whole-cell Kv1.2 currents were activated by depolarizing voltage steps from a holding potential of −90 mV, applied every 100 milliseconds, increasing each time by 10 mV, from −80 to +40 mV (ΔV). In the second set of experiments, Kv1.2 channel-mediated currents were recorded in the whole-cell patch-clamp configuration during 1-second depolarizing step to +60 mV from a holding potential of −80 mV. Recordings were carried out at room temperature using an Axopatch 1D amplifier (Axon Instruments, Foster City, CA, USA). Voltage command protocols and data acquisitions were performed by using pClamp 10.0 software and Digidata 1440A interface (Axon Instruments). Capacitive transients were neutralized and series resistance was monitored continuously throughout the experiment and compensated at 80% when indicated. If it changed by >20%, the cell was discarded. The voltage protocol encompassed a P/4 leak subtraction protocol. Data were filtered at 5 kHz and sampled at 10 kHz.

Viral vector injection in the CMT area and telemetric transmitter implantation

Male CD rats ($n = 16$) 2–2.5 months old (Charles River, Calco, Italy) were housed in a temperature- (23°C) and light- (12-h light/dark cycle) controlled environment, with commercial rodent pellets and water provided *ad libitum*. They were deeply anesthetized by intramuscular injection of 0.05 mg/kg medetomidine (Domitor, Pfizer, Milan, Italy), followed by a mix of 20 mg/kg tiletamine and zolazepam (Zoletil 100, Virbac, Milan, Italy). After anesthesia, animals received subcutaneous injection of 5 mg/kg anti-inflammatory carprofen (Rimadyl, Pfizer) and 150 mg/kg antibiotic Amoxicilin (Clamoxyl, Pfizer) and were mounted onto a stereotaxic device. The viral solution was delivered via 30-gauge stainless needle attached to a 10 μl Hamilton syringe with a motorized microinjector (Stoelting Co., Wood Dale, IL, USA). One microliter of AAV2/9-CMV-eGFP or AAV2/9-CMV-eGFP-2A-Kv1.2 vectors (1×10^{10} gc) was injected around the CMT area (coordinates of injection: anterioposterior −3.0 mm, lateral +1.7 mm with 13° tilt, dorsoventral −6.7 mm) at a rate of 0.2 μl/min. [Coordinates of injection were calculated from the Bregma level according to the Paxinos and Watson Rat Brain Atlas (IV edition) (Paxinos & Watson 2004)].

In addition, to collect the biopotential signals, a miniature multichannel telemetric transmitter (TL10M3-F40-EET, Data Sciences International, St. Paul, MN, USA) was implanted intraperitoneally into the animals. To allow recording of cortical EEG, two electrodes were fixed permanently, with dental cement, to the skull. They were directly in contact with the dura mater through two drilled holes on

the fronto-parietal region. Two electrodes were fixed to the skeletal muscles of the neck for recording electromyogram (EMG).

After recovery from surgery, animals were maintained in their home cage in a temperature-controlled environment (21 ± 1°C) with access to food and water *ad libitum*.

After the behavioural investigations, rat were killed, the brain frozen and then cut into 14 μm coronal slices with a cryostat (Leica Microsystems). The slices were collected on polarized glass slides (Menzel-Gläser, Braunschweig, Germany) and stored at −80°C for *in situ* hybridization and immunofluorescence.

A different batch of male CD rats ($n = 8$ per group), 1.5–2 months old (Charles River, Calco, Italy), were operated as described above for whole-cell patch-clamp recordings from acute brain slices (coordinates of injection: anterioposterior −2.6 mm, lateral +1.6 mm with 13° tilt, dorsoventral −6.5 mm).

All surgical procedures were performed under aseptic conditions and all procedures involving animals and their care were conducted in accordance with the local legislation (Legislative Decree No. 116, 27 January 1992), which acknowledged the European Communities Council Directive of 24 November 1986 86/609/EEC, and following the GlaxoSmithKline policy on the care and use of laboratory animals and related codes of practice.

Sleep recording and analysis

Implanted and injected animals showed normal behaviour immediately after recovery from surgery, but to allow normal sleep patterns to be re-established and to allow maximal AAV-mediated transgene expression, animals were evaluated after a three-week period. The environmental conditions described above were maintained throughout the sleep studies.

To evaluate the sleep profile of AAV-Kv1.2-transduced rats in comparison to AAV-GFP-transduced rats, EEG and EMG signals were recorded continuously using Dataquest® A.R.T. (Data Sciences International) for 24 h starting at the beginning of light period (circadian time 0). For the duration of the test period, freely moving animals remained in their home cages on individual receivers.

The EEG trace, divided into 10-second epochs, was digitally transformed (fast Fourier transformation) to provide the power spectra of δ, θ, α and β bands in order to distinguish three different activity patterns in the rat (awake, NREM sleep and rapid eye movement or REM sleep). The markers assigned by the automated scoring system (*Sleep stage*®, Data Science International) were transferred to the EEG digital signal and subsequently confirmed by visual examination of the EEG and EMG traces by trained operators, blinded to the drug treatment.

Analysis of sleep parameters included latency to NREM sleep (time interval to the first six consecutive NREM sleep epochs after injection), latency to REM sleep (time interval to the first REM sleep epoch after injection), NREM sleep, REM sleep and time awake (wake), number of episodes of awake, NREM and REM sleep, and brief awakening episodes defined as episodes of wake with a maximum length of 20 seconds.

Assessment of behaviour using the Laboras™ system

General behavioural activities of Kv1.2 and respective control rats (GFP) were investigated using the Laboras™ system (Laboratory Animals Behaviour Observation, Registration and Analysis System, Metris, Hoofddorp, the Netherlands). The Laboras™ system is an automatized system for the registration of behavioural activities in rodents (Quinn *et al*. 2003). To evaluate behaviour under physiological conditions, rats were acclimatized to LABORAS cages 12 h before starting registration and then behavioural activities were recorded for 24 h, starting at light on (0600 h). The following behaviours were recorded: immobility time, locomotor activity, grooming, climbing, food and water intake, undefined activities.

Whole-cell patch-clamp recordings from acute brain slices

For slice preparation, male CD rats were deeply anesthetized with isoflurane, typically 4–5 weeks after viral injections. The brain was quickly removed and immersed in oxygenated (95% O_2 – 5% CO_2) ice-cold artificial cerebrospinal fluid (ACSF) containing (in mM): 125 NaCl, 25 $NaHCO_3$, 2.5 KCl, 1.25 NaH_2PO_4, 1.2 $MgCl_2$, 2 $CaCl_2$, 25 Glucose, 1.7 L(+)-ascorbic acid. Coronal slices (300 μm) containing the CMT were cut on a vibratome and transferred to a holding chamber containing ACSF supplemented with myo-inositol (3 mM) and sodium pyruvate (2 mM). Slices were kept at 35°C for 30 min and then at room temperature for subsequent incubation.

Virally infected CMT neurons were visually identified using GFP fluorescence, excited via an OptoLED Lite (Cairn Research, Faversham, UK), and were typically located within paraventricular and intermediodorsal thalamic areas. Image acquisition was controlled via an Andor EM-CCD camera (Axon DU-897) and Andor Solis imaging software V. 4.16. Recordings were obtained with borosilicate micropipettes (TW150F-4, WPI) filled with (in mM): 140 $KMeSO_4$, 10 KCl, 10 HEPES, 0.1 EGTA, 4 Mg-ATP, 0.2 Na-GTP and 10 phosphocreatine (306 mOsm, pH 7.27). Membrane voltages were not corrected for liquid junction potential (measured value: −8 mV).

Whole-cell current-clamp recordings were performed at room temperature with a MultiClamp 700B amplifier driven by Clampex V. 10.2 (Molecular Devices, Wokingham, UK). Data were sampled at 5 kHz and filtered at 2 kHz. Bridge balance was compensated electronically. Off-line analysis was performed using Clampfit V. 10.2 (Molecular Devices).

Tonic action potential firing was elicited by square current steps (50–400 pA) from a membrane potential of −50 mV, whereas low-threshold bursts were activated at the offset of square hyperpolarizing current pulses, triggered from membrane potentials between −70 and −60 mV. Current commands hyperpolarizing the cell to at least −100 mV were used to trigger full-fledged low-threshold bursts. Changes in the resting membrane potential (RMP) during bath application of caffeine (20 mM, Sigma-Aldrich) were monitored for 10–19 min after the start of caffeine wash-in. The averaged RMP during 3 min of baseline and during the last 3 min in caffeine were statistically analyzed. Recovery after caffeine wash-out was monitored for 10–20 min.

Oligonucleotide radioactive in situ *hybridization*

An oligonucleotide probe complementary to rat Kv1.2 mRNA (5′-GGTAGTTGGAACCATGTCTCCATAGCCTACAGTTGTCATGGAG-3′) was designed and synthesized (Sigma-Aldrich). For each injected animal, two slides, each containing four brain slices, were used. The slides were incubated following the protocol described in Mugnaini *et al*. (2002). Finally, they were exposed to a Fuji imaging plate together with a ^{14}C standard for the quantification. The visualization and quantification of the autoradiogram were performed with the MCID V. 7.0 image analysis software (InterFocus Imaging, Linton, IN, USA).

Immunofluorescence staining

Frozen brain slices were processed for double immunofluorescence. Briefly, sections were fixed with acetone:methanol (50:50 v/v) solution for 15 min at −20°C and then washed three times in PBS (all reagents from Sigma). Then slides were incubated in PBS blocking solution containing 0.1% Triton-X-100, 3% normal goat serum (Vector Laboratories), 2% bovine serum albumin and 3% milk for 1 h, followed by overnight incubation in PBS blocking serum plus primary antibody at 4°C. The antibodies used were polyclonal Kv1.2 antibody 1:500 (see for details Koch *et al*. 1997) and monoclonal GFP antibody 1:500 (MAB3580, Chemicon).

Sections were then washed in PBS and incubated in secondary antibody (anti-mouse immunoglobulin/Alexa Fluor-488 and anti-rabbit immunoglobulin/Alexa Fluor-594, 1:1000, Molecular Probes) for 1 h, then mounted in Vectashield (Vector Laboratories) and coverslipped.

Images were acquired with the Nikon Microphot-Fxa fluorescence microscope at the 10× and 20× magnifications with the digital camera system Leica DC500 (Leica Microsystems) using the Leica IM50 (Version 1.20 – release 19) software.

Caffeine pharmacological treatment

Drug studies were carried out according to a randomized paired crossover design where, in separate experimental sessions, each animal received control and drug treatments. Animals were treated with caffeine or respective vehicle, in a volume of 2 ml/kg, at the beginning of light period (circadian time 0). Recordings were made for the subsequent 5-h test period. Caffeine was dissolved in saline solution (0.9% NaCl) and administered intraperitoneally (i.p.) in doses of 3 and 10 mg/kg.

Statistics

All data from the various experiments are presented in the graphs as mean values ± standard error of the mean (SEM). For the *in situ* hybridization experiment, *ex vivo* electrophysiology and the behavioural experiments under basal conditions, data were analyzed using the unpaired or paired *t*-test as appropriate. In the hybridization experiment, the relative Kv1.2 mRNA levels in the injected brains were calculated for each sample using the MCID V. 7.0 program (InterFocus Imaging) by expressing the mRNA level as density relative to [^{14}C] standards, and the statistical analysis has been conducted on logged density.

The effect of caffeine in AAV-Kv1.2- and AAV-GFP-injected rats has been analyzed through a mixed-effect model with treatment and gender (and their interaction) as fixed effects and rat as random effect, followed by least significant difference (LSD) *post hoc* tests.

Results

AAV2/9-CMV-eGFP-2A-Kv1.2 vector is able to express functional Kv1.2 protein in vitro

To show the ability of AAV2/9-CMV-eGFP-2A-Kv1.2 vector (hereafter referred to as AAV-Kv1.2) to express Kv1.2 protein, U2OS cells (a human osteosarcoma cell line) were infected with the viral vector expressing Kv1.2 or the GFP-expressing control vector AAV2/9-CMV-eGFP (hereafter referred to as AAV-GFP) at doses of 10^4, 10^5 or 10^6 gc/cell. High GFP expression was observed with 10^6 gc/cell of each vector, while very low or no GFP expression was observed with the 10^4 gc/cell dose (data not shown). The double fluorescent immunocytochemistry (ICC) analysis for GFP and Kv1.2 protein was performed in the U2OS infected with 10^6 gc/cell of AAV-GFP or AAV-Kv1.2. A clear Kv1.2 staining was detected in the AAV-Kv1.2-infected U2OS cells, while as expected, no specific staining was observed in the uninfected cells and in AAV-GFP-infected cells (Fig. 1a,b).

Infected U2OS cells at a dose of 10^6 gc/cell and control cells were analyzed by manual patch clamp to detect voltage-gated K^+ current in the Kv1.2-expressing cells, compatible with the expression of functional recombinant rat Kv1.2 channel. Two types of analyses were performed to characterize the current profile. Initially, the voltage-dependent activation of the K^+ current was investigated in the infected U2OS cells through whole-cell recordings by inducing depolarizing voltage steps. The extrapolation of the activation voltage of the K^+ current from the *I/V* plot showed that the activation voltage measured in the AAV-Kv1.2-infected cells (around −25 mV) is compatible with the Kv1.2 current profile reported in the literature for recombinant systems (Bähring *et al*. 2004; Papp *et al*. 2009; Zhu *et al*. 2009) (Fig. 1c,d).

Secondly, Kv1.2 channel-mediated currents were recorded in the whole-cell patch-clamp configuration to characterize the conductance profile of the K^+ current in the AAV-Kv1.2-infected cells. This analysis showed that the K^+ current recorded is characterized by a long activation time and a slow inactivation typical of the channel (Fig. 1e).

This further analysis confirms the presence of a voltage-gated K^+ current with the conductance profile of Kv1.2 current only in the AAV-Kv1.2-infected U2OS cells and not in the control cells. Other Kv1 channels exhibit similar current profiles; however, endogenous Kv1 channels are not expected to be expressed in this cell line.

Functional Kv1.2 protein is overexpressed in CMT after viral vector injection

A total of 10^{10} gc of AAV-Kv1.2 or the control AAV-GFP virus was injected stereotaxically in the rat CMT area. Two months after viral vector injection, rats were killed and the brain processed in order to detect the levels of Kv1.2 mRNA and protein. Kv1.2 mRNA expression was clearly increased in the central thalamic area of AAV-Kv1.2-injected rats (Fig. 2a,b), whereas Kv1.2 mRNA levels in the CMT of AAV-GFP-injected rats were comparable with the uninjected control animals (data not shown). The AAV-Kv1.2-injected rats showed a 42-fold increase in Kv1.2 mRNA expression compared to AAV-GFP-injected rats ($t_{15} = -24.6$, $P < 0.0001$; Fig. 2c). Indeed, Kv1.2 mRNA overexpression was clearly limited to the area of viral vector diffusion and around the needle track, thus confirming the ability of the viral vector to encode Kv1.2 mRNA. Viral vector diffusion was detected in the CMT area and in the surrounding thalamic regions such as part of the mediodorsal thalamic nuclei, the intermediodorsal thalamic area and in certain animals, the posterior part of the paraventricular thalamic nucleus.

Double immunofluorescence was performed in the injected slices to visualize rat Kv1.2 protein expression in CMT. Kv1.2 staining was clearly measured specifically in the AAV-Kv1.2-injected cells, with very low specific staining in the control-virus-injected brains (Fig. 2d–g).

To test for functional Kv1.2 overexpression in infected thalamic cells, we performed whole-cell patch-clamp recordings in acute slices prepared from animals injected with either AAV-GFP or AAV-Kv1.2 viral vectors. Strong GFP fluorescence in the injected areas led to unequivocal identification of neuron-like structures, in particular a large multipolar cell body and several thick dendritic processes (Fig. 2h). Patched cells showed RMPs of -67.0 ± 1.4 mV ($n = 14$) and -70.0 ± 1.4 mV ($n = 13$) for AAV-GFP and AAV-Kv1.2 expressions, respectively ($P > 0.05$), and overshooting action potentials upon depolarizing current injections (Fig. 2h). Moreover, cells from both groups showed action potential discharge superimposed on a triangular-shaped depolarizing wave at the offset of a hyperpolarizing current injection (Fig. 2i). This low-threshold burst capacity is a well-known property of excitatory thalamocortical cells.

Kv1.2 channel overexpression was assessed through monitoring tonic action potential discharge, induced through step depolarizing current injections (50–400 pA, 400 milliseconds). In GFP-expressing cells, stronger current injections typically led to gradually increasing action potential discharge. Saturating numbers of action potentials were, on

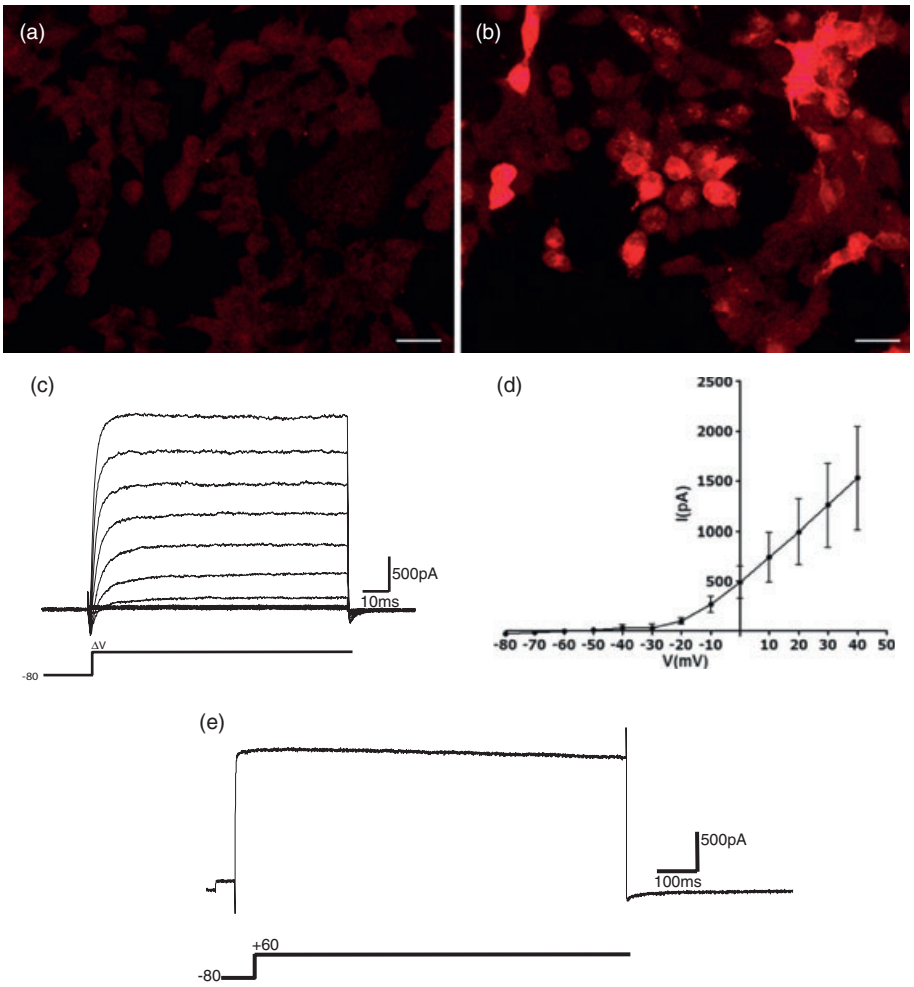

Figure 1: Functional Kv1.2 protein expression in U2OS. (a) Representative images showing Kv1.2 in U2OS cells infected with 10^6 gc/cell of AAV-eGFP or (b) AAV-Kv1.2 viruses detected by immunocytochemistry analysis. Scale bar: 50 μm. (c) Current families obtained in whole-cell recordings from U2OS cells infected with AAV-Kv1.2 virus ($\Delta V = -80$ to $+40$ mV). (d) *I*/*V* relationship obtained by plotting the peak of Kv1.2 current evoked against the different voltages applied. Data shown are the mean ± SEM of five cells per point. (e) Kv1.2-channel-mediated currents obtained during a 1-second depolarization to +60 mV from a holding potential of −80 mV, showing the slow inactivation typical of the channel.

average, reached around 250 pA (Fig. 2j). Limited discharge at these higher current injections resulted, at least in a considerable number of cells, from cumulative inactivation of action potentials. In Kv1.2-expressing cells, however, the steepness of this relation was markedly attenuated, with current injections remaining largely subthreshold up to ~200 pA, and weaker discharge at larger injections. The time–course of the action potentials was largely preserved in the two groups, including action potential threshold, peak and post-spike after hyperpolarization (Table S1), while the half-width of the spikes was shortened in the Kv1.2-overexpressing cells. These functional data substantiate the immunohistochemical demonstration of Kv1.2 overexpression by showing that this K^+ current principally antagonizes cell excitability by attenuating tonic discharge.

Normal behaviour and basal sleep profile are not altered after Kv1.2 overexpression in the CMT area

To evaluate circadian rhythms of Kv1.2-overexpressing rats in comparison with the GFP control group, behaviour and sleep profile were investigated in a familiar environment.

Behavioural activities were measured for 24 h using the Laboras™ system. Kv1.2 overexpression in the CMT area did not produce statistically significant variations in normal spontaneous behaviours in rats in either the dark phase or light phase (Table S2).

In addition, the basal sleep profile of Kv1.2 rats was investigated over 24 h. Kv1.2-overexpressing rats showed a normal sleep profile, without any statistically significant difference with respect to GFP control rats, in each of the sleep parameters measured during both the light phase ($t_{17} = -0.96$, $P = 0.35$ for NREM sleep; $t_{17} = 0.22$, $P = 0.82$ for REM sleep; $t_{17} = 0.52$, $P = 0.61$ for awake) and during dark phase ($t_{17} = -0.37$, $P = 0.71$ for NREM sleep; $t_{17} = 0.94$, $P = 0.36$ for REM sleep; $t_{17} = -0.25$, $P = 0.80$ for awake) (Fig. S1).

Viral vector-mediated rKv1.2 protein overexpression in rat CMT attenuates pro-arousal effect of caffeine

To analyze the effect of Kv1.2 overexpression during pharmacologically induced arousal, we studied the consequences of caffeine on sleep architecture and on *ex vivo* CMT neuron function. Animals were treated with 3 and 10 mg/kg caffeine

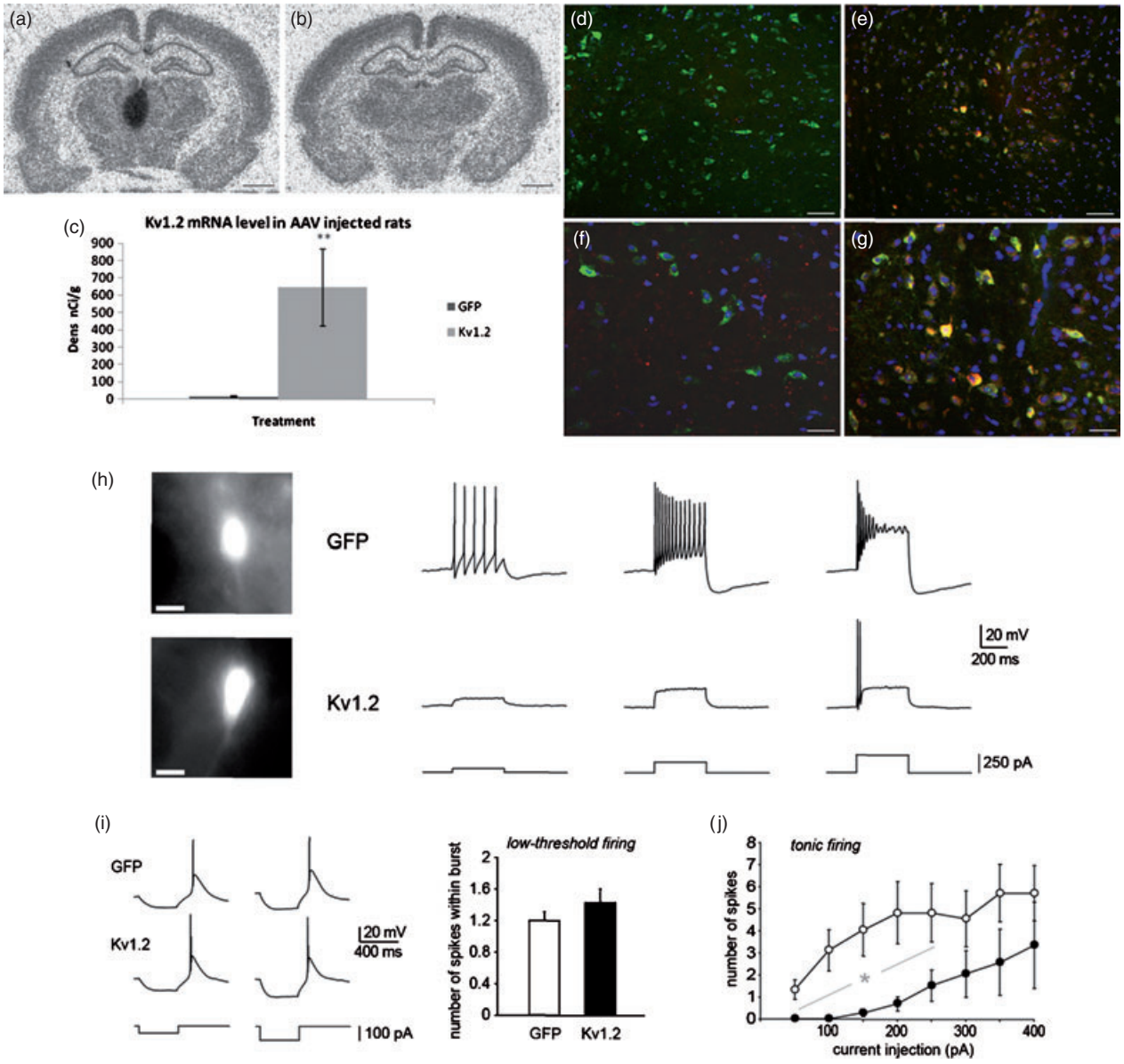

Figure 2: Kv1.2 channel expression in injected brains. (a) Kv1.2 mRNA expression in the brain of rats injected with 1 μl (1×10^{10} gc) of AAV-Kv1.2 virus or (b) AAV-eGFP virus detected by oligonucleotide *in situ* hybridization. Scale bar: 2 mm. (c) Quantification of Kv1.2 mRNA relative levels (expressed as nCi/g) in the AAV-eGFP- or AAV-Kv1.2-injected area (**$P < 0.01$). (d and f) Immunohistochemical analysis in the CMT of rats injected with 1 μl (1×10^{10} gc) of AAV-eGFP or (e and g) AAV-Kv1.2 viruses; red = Kv1.2, green = GFP, blue = DAPI, yellow = GFP-Kv1.2-co-expressing cells. Scale bar: 100 μm in d,e and 50 μm in f,g. (h) Tonic firing elicited in an AAV-GFP (GFP, *top traces*) and an AAV-Kv1.2 (*bottom traces*) CMT neuron (Kv1.2). Fluorescent images of the cell bodies are presented on the *left* (scale bars, 10 μm). Protocol schematically represented at the *bottom*, holding potential was −50 mV. Trains of action potentials were triggered in the GFP cell and displayed inactivation upon large depolarization. Fewer action potentials were elicited by large current injections in the Kv1.2-overexpressing cell. (i) Left, representative examples of low-threshold Ca^{2+} spikes elicited (protocol at the bottom, holding potential −60 mV). Right, summary plot of the average number of Na^{+} spikes crowning the low-threshold burst shows no significant difference between the two groups (GFP, $n = 15$; Kv1.2, $n = 14$; $P > 0.05$). (j) Mean relation between number of tonic action potentials and current injection. Note the larger number of action potentials generated in the GFP control cells compared to Kv1.2-overexpressing cells. Differences were significant for current steps between 50 and 250 pA (GFP, $n = 18$; Kv1.2, $n = 17$; *$P < 0.05$).

(doses selected on the basis of previous in-house studies and literature data; Paterson *et al*. 2007). The analysis of EEG and EMG traces over 5 h of observation indicated that caffeine, administered at the beginning of light phase, induced a dose-related increase of time spent awake (Fig. 3a). Analysis of variance showed a statistically significant treatment effect as well as treatment-group interaction effect (for treatment: $F_{2,24} = 88.98$, $P < 0.0001$; for treatment-group interaction: $F_{2,24} = 3.51$, $P = 0.046$). In particular, at the dose of 3 mg/kg, caffeine induced an increase in time spent awake reaching statistical significance in the GFP group ($P = 0.038$) and only marginally significant in the Kv1.2 group ($P = 0.08$). At the dose of 10 mg/kg, caffeine induced a robust increase in time spent awake both in GFP group and in Kv1.2 group ($P < 0.0001$). The comparison of Kv1.2 and GFP group showed that the pro-arousal effect induced by 10 mg/kg caffeine was significantly attenuated in Kv1.2 rats compared to GFP rats. In fact, while both Kv1.2 and GFP rats registered a significant increase in the total time spent awake over 5 h at the dose of 10 mg/kg compared to their controls, such an increase was approximately 30 min lower in Kv1.2 rats (for GFP rats, the difference between the 10 mg/kg caffeine group and vehicle is around 109 min, while for Kv1.2 rats it is estimated to be 75 min; the P value of the comparison is 0.023) (Fig. 3a).

The statistical analysis showed that 3 mg/kg caffeine induced a significant decrease of time spent in the REM phase compared to the vehicles, for both groups ($P = 0.04$ for GFP, $P = 0.05$ for Kv1.2 group) but not of the NREM phase ($P = 0.07$ for GFP, $P = 0.14$ for Kv1.2 group), while 10 mg/kg caffeine induced a robust decrease of time spent in REM and NREM phases in both groups ($P < 0.0001$) (Fig. 3c–f). Comparison between the Kv1.2 and the GFP groups confirmed the attenuated effect of caffeine in the Kv1.2 group with respect to GFP rats both in NREM and REM sleep at the dose of 10 mg/kg, but it reached statistical significance only in the NREM phase (mean in minutes ± SEM, GFP = 107.4 ± 9.9; Kv1.2 = 134.6 ± 11, $P = 0.018$).

Analysis of the time–course of the various sleep parameters provided evidence for a statistically significant effect of treatment, time and treatment by time interaction (for awake: $F_{\text{treatm } 2,36} = 61.67$, $P < 0.0001$; $F_{\text{time } 4,144} = 57.46$, $P < 0.0001$; $F_{\text{treatm*time } 8,144} = 10.40$, $P < 0.0001$; for NREM: $F_{\text{treatm } 2,36} = 71.14$, $P < 0.0001$; $F_{\text{time } 4,144} = 52.44$, $P < 0.0001$; $F_{\text{treatm*time } 8,144} = 10.36$, $P < 0.0001$; for REM $F_{\text{treatm } 2,36} = 5.49$, $P = 0.008$; $F_{\text{time } 4,144} = 26.21$,

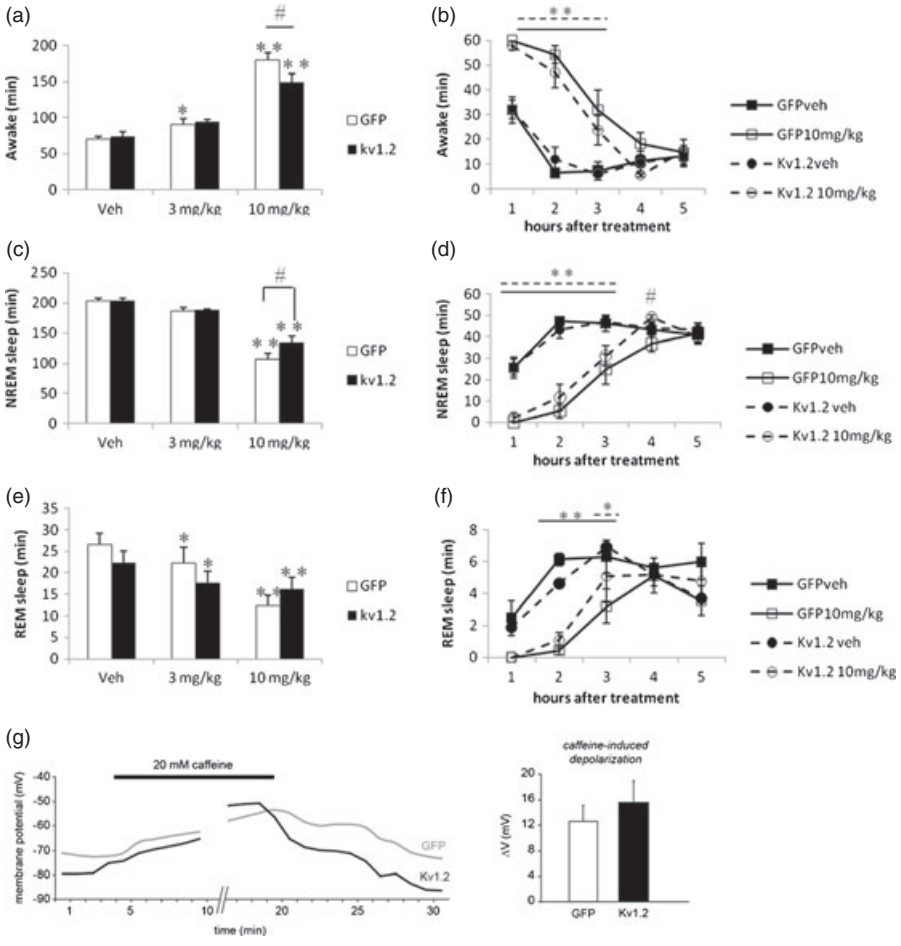

Figure 3: Effect of caffeine (3, 10 mg/kg i.p.) in Kv1.2 ($N = 6$) and GFP rats ($N = 8$) on sleep profile and caffeine effects (20 mM) on cellular membrane potential *in vitro*. Data are expressed as mean ± SEM. Total time spent in (a) awake, (c) NREM and (e) REM period over 5 h of observation and time–course during observation period for (b) awake, (d) NREM and (f) REM. *$P < 0.05$, **$P < 0.01$ of caffeine-treated group vs. respective vehicle group. #$P < 0.05$ of caffeine-treated Kv1.2 group with respect to GFP group. Dotted line: Kv1.2 group; straight line: GFP group. (g) Left, effect of bath application of 20 mM caffeine on the membrane potential of a GFP and a Kv1.2 cell. Right, pooled data of caffeine-induced depolarization (ΔV) show no difference (GFP, $n = 11$; Kv1.2, $n = 11$; $P > 0.05$).

$P < 0.0001$; $F_{\text{treatm*time } 8,144} = 2.38$, $P = 0.019$), while no other factors were statistically significant. In particular, awake and NREM duration in the 10 mg/kg caffeine-treated groups showed that the effect of caffeine (compared to vehicle) is statistically significant within the first 3 h of the experiment for both Kv1.2 and GFP groups; while in the REM sleep the differences to the controls are statistically significant on the second and third hour for the GFP group, and only on the third hour for the Kv1.2 group (Fig. 3b,d,f). In addition, on the fourth hour, a statistically significant difference in NREM sleep was registered between the Kv1.2 and GFP groups (Fig. 3d).

The analysis of sleep latency indicated that caffeine induced an increase in latency both for NREM ($F_{\text{treatm } 2,24} = 48.87$, $P < 0.0001$) and REM sleep ($F_{\text{treatm } 2,24} = 38.74$, $P < 0.0001$), statistically significant both in GFP and Kv1.2 rats at 3 ($P = 0.03$ for GFP, $P = 0.006$ for Kv1.2) and 10 mg/kg for NREM ($P < 0.0001$ for GFP and Kv1.2) sleep and at 10 mg/kg for REM sleep ($P < 0.0001$ for GFP and Kv1.2). No differences were observed between GFP and Kv1.2 (Fig. 4). Statistical analysis of the number of wake, NREM and REM episodes and of the brief awakenings (episodes of wake minor of 20 seconds) has been performed over the 5-h observation period. Even if small differences have been observed between Kv1.2 and GFP groups with caffeine at 3 mg/kg, it was not possible to make conclusive assumptions on alteration on sleep architecture because of the limited observation period (Table S3).

We finally tested effects of acute caffeine exposure at the cellular level. In slice preparations, bath application of caffeine (20 mM), a concentration within the range applied previously for *in vitro* studies (Budde *et al*. 2000; Parri & Crunelli 2003; Richter *et al*. 2005), induced a pronounced depolarization (ΔV) from RMP that was comparable between the two cell groups and reversible upon wash out (Fig. 3g). Therefore, Kv1.2-expressing neurons retained full sensitivity to this arousal-promoting drug in terms of the instantaneous electrical response.

Discussion

As previously described, several preclinical and clinical pieces of evidence suggest a role of the Kv1.2 channel in the regulation of sleep and arousal profile. Nonetheless, no previous investigations of the effect of Kv1.2 activation on sleep profile in rodents have been reported. To overcome the lack of pharmacological agents, we employed viral vector-mediated Kv1.2 channel overexpression in the rat CMT. Using this approach, we showed that Kv1.2 overexpression significantly decreased caffeine-induced effects on arousal and NREM sleep, without affecting sleep parameters under normal physiological conditions.

Our data show that viral vector-mediated Kv1.2 overexpression induced a significant reduction of neuronal excitability in the infected CMT excitatory neurons. This effect was particularly pronounced for tonic action potential discharge of infected neurons, which is typically shaped by delayed rectifier K^+ currents of the Kv1 type and thus consistent with an overexpression of Kv1.2 channels. In contrast, the burst mode of discharge seemed unaltered, consistent with a minor role of Kv1-type K^+ currents in this type of electrical excitability. In spite of these pronounced modifications at the cellular level, we did not observe changes in normal spontaneous behaviour and sleep profile in the basal condition between Kv1.2-overexpressing and AAV-GFP-injected control animals, as measured by Laboras™ and polysomnography studies. Further studies will be required to understand in more detail the discharge patterns in CMT neurons, and possibly associated Kv1.2 activation, which correlate with different states of vigilance.

To investigate the role played by Kv1.2 overexpression in a condition of sleep disturbance and increased arousal, caffeine treatment was employed to produce a translational model of insomnia in rats, because of the similar effects produced on sleep profile in humans and rodents (Paterson *et al*. 2007). In particular, as shown in our study, caffeine treatment increases wakefulness and decreases total sleep time in treated rats. Adeno-associated-viral-vector-injected animals were treated with two different doses of caffeine, 3 and 10 mg/kg or with the vehicle; 3 mg/kg of caffeine induced a significant but very small effect only on certain sleep parameters while 10 mg/kg caffeine induced a strong and significant increase in the time spent awake and decrease in the duration of NREM and REM in both AAV-injected groups. Therefore, in order to analyze if Kv1.2 overexpression protects against caffeine-induced sleep disturbance in rats, 10 mg/kg was the preferred dose; in fact this caffeine amount is also reported in the literature as a preferred dose to study the efficacy of sleep-promoting medications in rodents. In the literature, 10 mg/kg caffeine is reported to produce in rat many of the signs of insomnia observed in humans and these symptoms improved after treatment of the animals with zolpidem and trazodone,

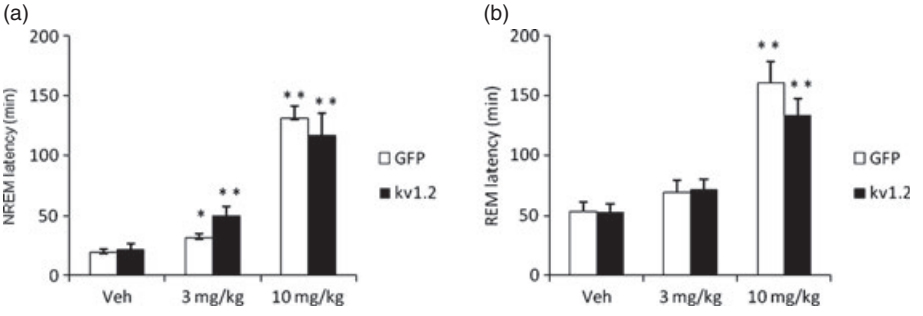

Figure 4: Effect of caffeine (3, 10 mg/kg i.p.) in Kv1.2 ($N = 6$) and GFP rats ($N = 8$) on sleep onset. Data are expressed as mean ± SEM. (a) NREM latency and (b) REM latency $*P < 0.05$, $**P < 0.01$ of caffeine-treated group vs. respective vehicle group.

two of its most successful current medications (Paterson *et al*. 2009).

In our studies, we showed that animals injected with the targeting vector AAV-Kv1.2 in the CMT area spent significantly less time awake after 10 mg/kg caffeine treatment (34 min less) and significantly more time in NREM phase (roughly 30 min more) compared with the control-virus-injected animals. No statistically significant difference was observed in the REM phase, even if there was a trend for REM increase in the Kv1.2 group. It is interesting to note that our results are in line with the alterations on sleep profile observed in Kv1.2 KO mice in basal conditions, even if we cannot directly compare our model with the KO mice (Douglas *et al*. 2007). Kv1.2 KO mice showed a significant increase in time spent awake and reduction in the duration of NREM phase compared with the wild-type animals, while no statistically significant difference was reported in the REM period. This sleep profile in basal condition suggests an increased level of arousal in mice in which Kv1.2 channel is completely absent. In fact, the constitutive genetic disruption of Kv1.2 is likely to strongly reduce functional Kv1 heterotetrameric channels with a significant increase in the basal level of neuronal excitability. In agreement, we showed that Kv1.2 overexpression in the CMT protects from NREM disruption and increased arousal after caffeine treatment in rats. These results seem to indicate a potential role of Kv1.2 in acting as a filter in the control of arousal level and in contrasting excessive activation of arousal pathways. In agreement with these results, analysis of the time–course of awake and NREM duration in the 10 mg/kg caffeine-treated groups suggests that Kv1.2 overexpression facilitates restoration of a normal sleep profile compared with the GFP control group. The question remained whether these differences arose from altered caffeine sensitivity in the Kv1.2-overexpressing cells. Contrary to this idea, we found that caffeine treatment (20 mM) induced a comparable depolarization in both control and Kv1.2-overexpressing cells, indicating that basic caffeine effects at RMPs were preserved. However, as discussed above, Kv1.2-overexpressing neurons showed decreased excitability in response to somatic current injections. Therefore, an attenuated synaptically mediated recruitment of CMT cells during sleep–wake transition could explain the observed decrease in wake duration with caffeine.

The effect of caffeine on sleep is thought to be mediated largely by the central antagonism of the adenosine sleep-promoting action, mainly through A2A receptors, which result in the activation at several levels of the ascending arousal system (Huang *et al*. 2005; Paterson *et al*. 2009). Adenosine is believed to control sleep homeostasis through inhibition of the histaminergic arousal system and through modulation of the release of several neurotransmitters such as glutamate and serotonin (Nehlig *et al*. 1992). Kv1.2 is a voltage-gated potassium channel with a subthreshold voltage range which, through mediating membrane hyperpolarization, reduces neuronal excitation (Guan *et al*. 2006). This activity could therefore contrast the neuronal hyperexcitation induced by pro-arousal substances such as caffeine and facilitate the restoration of normal arousal level (Radulovacki 1985). Moreover, because of their peculiar kinetic and conductance profile, neuronal Kv1.x currents could also contribute by regulating the depolarized holding potentials in awake behaving animals (Steriade *et al*. 2001). In mammal brains, high Kv1.2 expression is reported in the thalamocortical area which plays an important role in the control of sleep rhythms (Kues & Wunder 1992). We showed that localized Kv1.2 overexpression in a limited area of CMT was sufficient to induce a significant protecting effect against caffeine-induced activation of arousal pathways. This result supports the hypothesis that the CMT plays an important role in regulating sleep profile. The CMT area connects with brainstem areas, mediating arousal, and projects to wide cortical region and basal ganglia areas (Lydic & Baghdoyan 2005; Miller *et al*. 1989). Therefore, CMT interacts with both ascending (from brainstem) and descending (from cortex) arousal pathways (Alkire *et al*. 2009). On the basis of this fact, Kv1.2 channels located in the CMT region may have an important role in mediating transmission of information to the cortex, in order to control the level of activation of the arousal pathways. It is noted that AAV-mediated Kv1.2 mRNA overexpression was detected also in the surrounding thalamic area that could also have contributed at contrasting the effect of caffeine-mediated arousal.

In conclusion, viral vector-mediated Kv1.2 overexpression in the CMT area significantly attenuated the effect of 10 mg/kg caffeine on sleep profile, in particular the increase in time spent awake and the reduced time in NREM. As no effects were observed in basal conditions, we can conclude that the results reported are not due to non-specific effects on general behaviours. Our studies support previous reports, suggesting the role of Kv1.2 channels in contributing to sleep physiology (Alkire *et al*. 2009; Douglas *et al*. 2007) and show the ability of Kv1.2 to control the level of arousal in conditions of sleep disturbance. Our data may therefore suggest a potential therapeutic role of Kv1.2 activators in promoting sleep induction and maintenance in the condition of pathological sleep disturbance such as insomnia. Kv1.2 channel activation may in fact represent a protective mechanism against neuronal hyperexcitability and increased arousal levels associated with certain insomnia states. This hypothesis needs to be further investigated through the development and validation of Kv1.2-specific activators. Moreover, because of the possible contribution of other Kv1.x channels in producing the final functional Kv1.2 channel in the brain, ideal positive activator compounds would require to be specific for centrally expressed Kv1.x channels.

References

Alkire, M.T., Asher, C.D., Franciscus, A.M. & Hahn, E.L. (2009) Thalamic microinfusion of antibody to a voltage-gated potassium channel restores consciousness during anesthesia. *Anesthesiology* **110**, 766–773.

Bähring, R., Vardanyan, V. & Pongs, O. (2004) Differential modulation of Kv1 channel-mediated currents by co-expression of Kvbeta3 subunit in a mammalian cell-line. *Mol Membr Biol* **21**, 19–25.

Budde, T., Sieg, F., Braunewell, K.H., Gundelfinger, E.D. & Pape, H.C. (2000) Ca^{2+}-induced Ca^{2+} release supports the relay mode of activity in thalamocortical cells. *Neuron* **26**, 483–492.

Bushey, D., Huber, R., Tononi, G. & Cirelli, C. (2007) Drosophila Hyperkinetic mutants have reduced sleep and impaired memory. *J Neurosci* **27**, 5384–5393.

Cirelli, C. (2009) The genetic and molecular regulation of sleep: from fruit flies to humans. *Nat Rev Neurosci* **10**, 549–560.

Cirelli, C., Bushey, D., Hill, S., Huber, R., Kreber, R., Ganetzky, B. & Tononi, G. (2005) Reduced sleep in Drosophila Shaker mutants. *Nature* **434**, 1087–1092.

Douglas, C., Vyazovskiy, V., Southard, T., Faraguna, U., Cirelli, C. & Tononi, G. (2006) Voltage-dependent potassium channels Kv1.2: effects on sleep and EEG power spectrum of intracortical injections of an anti-kv1.2 antibody. *Sleep* **29** (Suppl.), A36.

Douglas, C.L., Vyazovskiy, V., Southard, T., Chiu, S.Y., Messing, A., Tononi, G. & Cirelli, C. (2007) Sleep in Kcna2 knockout mice. *BMC Biol* **5**, 42.

Gao, G.P., Alvira, M.R., Wang, L., Calcedo, R., Johnston, J. & Wilson, J.M. (2002) Novel adeno-associated viruses from rhesus monkeys as vectors for human gene therapy. *Proc Natl Acad Sci U S A* **99**, 11854–11859.

Guan, D., Lee, J.C., Tkatch, T., Surmeier, D.J., Armstrong, W.E. & Foehring, R.C. (2006) Expression and biophysical properties of Kv1 channels in supragranular neocortical pyramidal neurones. *J Physiol* **571**, 371–389.

Gutman, G.A., Chandy, K.G., Adelman, J.P. *et al*. (2003) International Union of Pharmacology. XLI. Compendium of voltage-gated ion channels: potassium channels. *Pharmacol Rev* **55**, 583–586.

Huang, Z.L., Qu, W.M., Eguchi, N., Chen, J.F., Schwarzschild, M.A., Fredholm, B.B., Urade, Y. & Hayaishi, O. (2005) Adenosine A2A, but not A1, receptors mediate the arousal effect of caffeine. *Nat Neurosci* **8**, 858–859.

Kleopa, K.A., Elman, L.B., Lang, B., Vincent, A. & Scherer, S.S. (2006) Neuromyotonia and limbic encephalitis sera target mature Shaker-type K+ channels: subunit specificity correlates with clinical manifestations. *Brain* **129**, 1570–1584.

Koch, R.O., Wanner, S.G., Koschak, A., Hanner, M., Schwarzer, C., Kaczorowski, G.J., Slaughter, R.S., Garcia, M.L. & Knaus, H.G. (1997) Complex subunit assembly of neuronal voltage-gated K+ channels. Basis for high-affinity toxin interactions and pharmacology. *J Biol Chem* **272**, 27577–27581.

Koh, K., Joiner, W.J., Wu, M.N., Yue, Z., Smith, C.J. & Sehgal, A. (2008) Identification of SLEEPLESS, a sleep-promoting factor. *Science* **321**, 372–376.

Kues, W.A. & Wunder, F. (1992) Heterogeneous expression patterns of mammalian potassium channel genes in developing and adult rat brain. *Eur J Neurosci* **4**, 1296–1308.

Liguori, R., Vincent, A., Clover, L., Avoni, P., Plazzi, G., Cortelli, P., Baruzzi, A., Carey, T., Gambetti, P., Lugaresi, E. & Montagna, P. (2001) Morvan's syndrome: peripheral and central nervous system and cardiac involvement with antibodies to voltage-gated potassium channels. *Brain* **124**, 2417–2426.

Lydic, R. & Baghdoyan, H.A. (2005) Sleep, anesthesiology, and the neurobiology of arousal state control. *Anesthesiology* **103**, 1268–1295.

Miller, J.W., Hall, C.M., Holland, K.D. & Ferrendelli, J.A. (1989) Identification of a median thalamic system regulating seizures and arousal. *Epilepsia* **30**, 493–500.

Mugnaini, M., Tessari, M., Tarter, G., Merlo Pich, E., Chiamulera, C. & Bunnemann, B. (2002) Upregulation of [3H]methyllycaconitine binding sites following continuous infusion of nicotine, without changes of alpha7 or alpha6 subunit mRNA: an autoradiography and in situ hybridization study in rat brain. *Eur J Neurosci* **16**, 1633–1646.

Nehlig, A., Daval, J.L. & Debry, G. (1992) Caffeine and the central nervous system: mechanisms of action, biochemical, metabolic and psychostimulant effects. *Brain Res Rev* **17**, 139–170.

Papp, F., Batista, C.V., Varga, Z., Herceg, M., Román-González, S.A., Gaspar, R., Possani, L.D. & Panyi, G. (2009) Tst26, a novel peptide blocker of Kv1.2 and Kv1.3 channels from the venom of Tityus stigmurus. *Toxicon* **54**, 379–389.

Parri, H.R. & Crunelli, V. (2003) The role of Ca^{2+} in the generation of spontaneous astrocytic Ca^{2+} oscillations. *Neuroscience* **120**, 979–992.

Paterson, L.M., Wilson, S.J., Nutt, D.J., Hutson, P.H. & Ivarsson, M. (2007) A translational, caffeine-induced model of onset insomnia in rats and healthy volunteers. *Psychopharmacology (Berl)* **191**, 943–950.

Paterson, L.M., Wilson, S.J., Nutt, D.J., Hutson, P.H. & Ivarsson, M. (2009) Characterisation of the effects of caffeine on sleep in the rat: a potential model of sleep disruption. *J Psychopharmacol* **23**, 475–486.

Paxinos, G. & Watson, C. (2004) *The Rat Brain in Stereotaxic Coordinates*, 4th edn. Academic Press, New York.

Quinn, L.P., Stean, T.O., Trail, B., Duxon, M.S., Stratton, S.C., Billinton, A. & Upton, N. (2003) LABORAS: initial pharmacological validation of a system allowing continuous monitoring of laboratory rodent behaviour. *J Neurosci Methods* **130**, 83–92.

Radulovacki, M. (1985) Role of adenosine in sleep in rats. *Rev Clin Basic Pharm* **5**, 327–339.

Richter, T.A., Kolaj, M. & Renaud, L.P. (2005) Low voltage-activated Ca^{2+} channels are coupled to Ca^{2+}-induced Ca^{2+} release in rat thalamic midline neurons. *J Neurosci* **25**, 8267–8271.

Steriade, M. (2006) Grouping of brain rhythms in corticothalamic systems. *Neuroscience* **137**, 1087–1106.

Steriade, M., Timofeev, I. & Grenier, F. (2001) Natural waking and sleep states: a view from inside neocortical neurons. *J Neurophysiol* **85**, 1969–1985.

Trimmer, J.S. & Rhodes, K.J. (2004) Localization of voltage-gated ion channels in mammalian brain. *Annu Rev Physiol* **66**, 477–519.

Wu, M.N., Joiner, W.J., Dean, T., Yue, Z., Smith, C.J., Chen, D., Hoshi, T., Sehgal, A. & Koh, K. (2010) SLEEPLESS, a Ly-6/neurotoxin family member, regulates the levels, localization and activity of Shaker. *Nat Neurosci* **13**, 69–75.

Wulff, H., Castle, N.A. & Pardo, L.A. (2009) Voltage-gated potassium channels as therapeutic targets. *Nat Rev Drug Discov* **8**, 982–1001.

Zhu, J., Recio-Pinto, E., Hartwig, T., Sellers, W., Yan, J. & Thornhill, W.B. (2009) The Kv1.2 potassium channel: the position of an N-glycan on the extracellular linkers affects its protein expression and function. *Brain Res* **1251**, 16–29.

Acknowledgments

The authors would like to thank Dr Marcelo Rosato Siri for valuable scientific discussion. This work was supported by a Hungarian Eötvös Scholarship to Z.R., by the Synapsis Foundation (S.A.) and by the Swiss National Science Foundation (A.L.).

Supporting Information

Additional Supporting Information may be found in the online version of this article:

Figure S1: Sleep profile of Kv1.2 ($N = 9$) and GFP rats ($N = 10$). Data are expressed as mean ± SEM of time spent awake (a,b), NREM sleep (c,d), REM sleep (e,f). Graphics a, c and e represent total time spent in sleep phase during light and dark phases; graphics b, d and f represent time–course of sleep profile during 24 h of observation.

Table S1: Action potential characteristics and post-spike after hyperpolarization (AHP) of cells during tonic discharge (GFP, $n = 18$; Kv1.2, $n = 17$; $^*P < 0.05$).

Table S2: Behavioural profile of Kv1.2 ($N = 10$) and GFP rats ($N = 10$). Data are expressed as mean (min) ± SEM of time in each behaviour over 12 h of light period (LD) and 12 h of dark period (DP).

Table S3: Effects of caffeine administered at 3 and 10 mg/kg i.p. in GFP and Kv1.2 rats during light phase (starting time CT0). Values are expressed as mean of *N* of episodes ± SEM ($n = 8$). $^{*}P < 0.05$, $^{**}P < 0.01$ for each dose vs. corresponding vehicle; $\#\#P < 0.01$ for Kv1.2 gender vs. GFP.

As a service to our authors and readers, this journal provides supporting information supplied by the authors. Such materials are peer-reviewed and may be re-organized for online delivery, but are not copy-edited or typeset. Technical support issues arising from supporting information (other than missing files) should be addressed to the authors.